

**Transverse momentum resummation effects in  $W^+W^-$  measurements**Patrick Meade,<sup>\*</sup> Harikrishnan Ramani,<sup>†</sup> and Mao Zeng<sup>‡</sup>*C. N. Yang Institute for Theoretical Physics, Stony Brook University, Stony Brook, New York 11794, USA*

(Received 8 September 2014; published 1 December 2014)

The  $W^+W^-$  cross section has remained one of the most consistently discrepant channels compared to Standard Model (SM) predictions at the LHC, measured by both ATLAS and CMS at 7 and 8 TeV. Developing a better modeling of this channel is crucial to understanding properties of the Higgs and potential new physics. In this paper we investigate the effects of next-to-next-to-leading-log transverse momentum resummation in measuring the  $W^+W^-$  cross section. In the formalism we employ, transverse momentum resummation does not change the total inclusive cross section but gives a more accurate prediction for the  $p_T$  distribution of the diboson system. By reweighting the  $p_T$  distribution of events produced by Monte Carlo generators, we find a systematic shift that decreases the experimental discrepancy with the SM prediction by approximately 3%–7% depending on the Monte Carlo generator and parton shower used. The primary effect comes from the jet-veto cut used by both experiments. We comment on the connections to jet-veto resummation and other methods the experiments can use to test this effect. We also discuss the correlation of resummation effects in this channel with other diboson channels. Ultimately  $p_T$  resummation improves the agreement between the SM and experimental measurements for most generators but does not account for the measured  $\sim 20\%$  difference with the SM, and further investigations into this channel are needed.

DOI: [10.1103/PhysRevD.90.114006](https://doi.org/10.1103/PhysRevD.90.114006)

PACS numbers: 12.38.-t, 12.38.Cy, 12.38.Qk

**I. INTRODUCTION**

The Standard Model (SM) of particle physics has been tested at a new energy frontier by the Large Hadron Collider (LHC). SM cross sections were measured at both 7 and 8 TeV, and the SM has passed with flying colors in almost every channel. Nevertheless there has been one channel that has been consistently off at the LHC for both the ATLAS and CMS experiments, the  $W^+W^-$  cross section measured in the fully leptonic final state. This state is naively one of the most straightforward channels to measure both theoretically and experimentally as it is an electroweak final state with two hard leptons. However, at 7 and 8 TeV ATLAS [1,2] and CMS [3,4] have measured a discrepancy with the SM next-to-leading-order (NLO) calculation [5,6] of  $\mathcal{O}(20\%)$ , and this extends to differential measurements not just simply an overall rescaling.

This discrepancy is particularly compelling for a number of reasons. First and foremost, one of the most important channels for the Higgs is the  $W^+W^-$  decay channel of which SM  $W^+W^-$  is the largest background. Since this channel does not have a particular kinematic feature akin to bumps in the  $\gamma\gamma$  or  $ZZ$  channels, it is important to understand the shape of the SM background quite well. CMS [7] and ATLAS [8] use data-driven techniques to extrapolate and find the signal strength of the Higgs. While these data-driven techniques are validated in many ways, it is oftentimes difficult to find perfectly orthogonal

control regions, and correlations may arise at higher order in theoretical calculations or because of new physics contributions. Given the shape differences observed, whether or not this is due to an insufficient SM calculation or new physics, it is important to understand that there could possibly be effects which alter the signal strength of the Higgs when the SM  $W^+W^-$  channel is understood better [9].

Another compelling reason for understanding the discrepancy is the possibility of new sub-TeV scale physics. The dilepton + missing transverse energy (MET) final state is an important background to many searches, but even more so, the large  $\mathcal{O}(\text{pb})$  discrepancy currently observed still allows for the possibility of new  $\mathcal{O}(100)$  GeV particles. While models of this naively would have been ruled out by previous colliders, or other searches at the LHC, in fact it turns out that there could be numerous possibilities for physics at the electroweak (EW) scale. These include Charginos [10], Sleptons [11], Stops [12–14] or even more exotic possibilities [15]. Remarkably, as first shown in Ref. [10], not only could new physics be present at the EW scale, but it in fact can *improve* the fit to data compared to the SM significantly, because it preferentially fills in gaps in the differential distributions when new physics is at the EW scale. In particular the possibility of particles responsible for naturalness in supersymmetry being at the weak scale and realizing a solution of the hierarchy problem makes this particularly compelling given all the negative results in other channels.

Finally, it is particularly interesting simply from the point of QCD and the SM to understand why the  $W^+W^-$  channel has a persistently discrepant experimental result compared

<sup>\*</sup>meade@insti.physics.sunysb.edu<sup>†</sup>hramani@insti.physics.sunysb.edu<sup>‡</sup>mao.zeng@stonybrook.edu

to SM predictions when other similar uncolored final states, e.g.  $ZZ$  and  $WZ$ , seem to agree quite well with experiment. There are potential theoretical reasons within the SM that could explain the difference compared to experiment and to other EW channels. One of the first points that could be addressed in the context of the  $W^+W^-$  measurement is whether or not the fixed-order calculation was sufficient to describe the data. Currently the  $W^+W^-$  channel is formally known at NLO, and this is implemented in various NLO Monte Carlo (MC) generators employed by ATLAS and CMS in their analyses. However, partial next-to-next-to-leading-order (NNLO) results are also incorporated, since  $gg \rightarrow W^+W^-$  via a quark loop is included through the generator gg2VV [16,17]. The merging of NLO WW and WWj predictions has been investigated in Refs. [18–20], while approximate calculations for higher-order corrections to  $gg \rightarrow W^+W^-$  are performed in Ref. [21]. Theoretically the full NNLO calculation of  $W^+W^-$  production turns out to be quite difficult, but within the past year there has been a great deal of progress; the complete NNLO calculation for the  $ZZ$  total cross section has recently been completed [22]. The results of Ref. [22] are interesting, given that compared to NLO the NNLO effect can be sizable  $\mathcal{O}(10\%)$ . However, when examined closely, if the full NNLO results are compared to the NLO +  $gg \rightarrow ZZ$ , the difference is less than  $\mathcal{O}(5\%)$ . Given this result for  $ZZ$ , unless there were large differences from a channel with very similar contributions, it would be highly unlikely that the full NNLO result could explain the discrepancies in the  $W^+W^-$  result.

There can be effects beyond the fixed-order calculation that matter as well. As with any calculation there are additional logarithms that arise whenever there is an extra scale in the problem, for instance threshold resummation logs, or logs of the transverse momentum of the system compared to the hard scale of the system. These logarithms can either change the overall cross section as in the case of threshold resummation or the shape of the  $p_T$  distribution in  $p_T$  resummation. In Ref. [23] the threshold resummation effects were calculated to approximate next-to-next-to-leading-log (NNLL) accuracy for  $W^+W^-$  production, and the effects were found to be small for the overall cross section of  $\mathcal{O}(.5-3\%)$  compared to NLO (the NNLO calculation would largely include these logs, and thus these effects should not be taken independently in magnitude). Another contribution which primarily affects the overall cross section comes from  $\pi^2$  resummation [24–26]. This has yet to be computed for  $W^+W^-$ ; however, it would affect other EW channels similarly, so the  $W^+W^-$  channel should not be singled out, and it clearly does not explain a discrepancy of  $\mathcal{O}(20\%)$  as measured in that channel.

While the aforementioned effects primarily affect the total cross-section, there are avenues that change the shape in a differential direction while keeping the total cross

section constant. One such effect is  $p_T$  resummation first calculated for  $W^+W^-$  in Refs. [27,28]. An interesting difference that arises with  $p_T$  resummation, compared to threshold resummation, is the interplay between the effects of resummation and the way the cross section is measured for  $W^+W^-$ . Given that  $p_T$  resummation changes the shape of the  $p_T$  distribution, and the  $p_T$  distribution would be a delta function at 0 at the Born level, QCD effects are crucial for getting this distribution correct. These effects are normally sufficiently accounted for by using a parton shower [matched to leading order (LO) or NLO fixed order] which only approaches next-to-leading-log (NLL) accuracy. However, in the  $W^+W^-$  channel compared to the  $W^\pm Z$  and  $ZZ$  channels there is an additional jet-veto requirement for the measurement. This requirement arises because there is an overwhelming background to  $W^+W^-$  coming from  $t\bar{t}$  production and decay. The most straightforward way to reduce the  $t\bar{t}$  background is to veto on extra jets to isolate the  $W^+W^-$  contribution. Given this jet veto, and the correlation between jet-veto efficiency and the  $p_T$  shape of the  $W^+W^-$  system, there is an added sensitivity to the jet veto and the shape of the  $p_T$  distribution that other channels typically do not have. There is precedent for turning to  $p_T$  resummation rather than using a parton shower alone when shape differences are important, e.g. the W mass measurement at the D0 [29].

In this paper we will examine the detailed effects of  $p_T$  resummation at approximate NNLL accuracy when combined with how the experimental measurements are performed. Typically the comparison between  $p_T$  resummed processes, e.g. Drell-Yan or  $ZZ$ , is done at the unfolded level experimentally. However, the extrapolation from the fiducial cross section to the inclusive cross section can be the source of the discrepancy, and a new analysis has to be carefully performed to understand the  $W^+W^-$  channel. The difficulty in doing this of course is that in the context of  $p_T$  resummation all radiation is inclusively summed without reference to a jet algorithm, and there is no jet veto that can be explicitly performed. In light of this, we undertake a procedure similar to what is done for Higgs production predictions at the LHC using HqT [30] to predict the transverse momentum distribution of the Higgs. We investigate the effects of taking NLO + parton shower generated events for  $W^+W^-$ , reweighting them with the NNLL resummed  $p_T$  distribution before cuts and then applying the cuts to find the fiducial cross section and how the total cross section should be interpreted. We find that this leads to  $\mathcal{O}(3-7\%)$  changes in the total cross section, for central choices of scales, which reduces the discrepancy. Additionally, we find that differential distributions are improved.

A jet veto introduces an additional scale and thus logs related to this scale. Such logs are not identical to the logs accounted for by  $p_T$  resummation. A program of jet-veto resummation [31–38] would in principle be required to

isolate these effects. These logs are clearly not taken account in our calculation explicitly due to the fact that there are no jets in our resummation calculation. Nevertheless, as mentioned earlier, the probability of an event passing the jet veto and the transverse momentum of the  $W^+W^-$  system is strongly correlated; therefore, in the process of reweighting the parton showered events and using a jet algorithm, there is a large overlap between the logs accounted for in jet-veto resummation and the logs accounted for in our procedure. This correlation was observed for instance in Ref. [31], where for Higgs and Drell-Yan the effects of reweighting the  $p_T$  distribution agreed very well with the jet-veto efficiency coming from a jet-veto resummation calculation. Given that Higgs production is dominated by gluon initial states, we expect the agreement between reweighting and jet-veto resummation to be even better for  $W^+W^-$ . An additional motivation for performing  $p_T$  resummation and reweighting is that we can perform detector simulations on the fully exclusive events and predict differential observables. In particular, the  $p_T$  distribution of the  $W^+W^-$  system, which ATLAS has shown at 7 and 8 TeV, has had a shape discrepancy which we find is in better agreement when performing  $p_T$  resummation. In the context of a jet-veto resummation calculation alone it is impossible to predict this shape without resorting to a reweighting procedure as well. Nevertheless, it would be interesting to understand the interplay of jet veto and  $p_T$  resummation effects even further, which we leave to future work.

The rest of the paper is structured as follows. In Sec. II, we outline our methodology and calculation of the NNLL resummed  $W^+W^-$   $p_T$  distribution. In Sec. III we explicitly describe our reweighting procedure and demonstrate the effects on the total cross section at various energies from different NLO generators and parton showers. Finally, in Sec. IV we discuss the implications of these results both for scale choices used in resummation and the associated errors as well as how to test these effects in other channels. In particular, given the similarity in scales of  $W^+W^-$ ,  $W^\pm Z$  and  $ZZ$  processes and the fact that resummation does not differentiate with respect to the hard matrix element, if resummation effects are responsible for even part of the discrepancy as currently measured there are distinct predictions in other channels.

## II. $W^+W^-$ TRANSVERSE MOMENTUM RESUMMATION

### A. Resummation method

For hadron collider production of electroweak bosons with invariant mass  $M$  and transverse momentum  $p_T$ , the fixed-order perturbative expansion acquires powers of large logarithms,  $\alpha_s^n \log^m(M/p_T)$ , with  $m \leq 2n - 1$ , which can be resummed to all orders [39–48]. We implement the method of Refs. [49,50] to calculate the  $WW$  transverse

momentum distribution at partial NNLL + LO.<sup>1</sup> Some aspects of the method are outlined below. The factorized cross section is

$$\begin{aligned} \frac{d\sigma^{WW}}{dp_T^2}(p_T, M, s) &= \sum_{a,b} \int_0^1 dx_1 \int_0^1 dx_2 f_{a/h_1}(x_1, \mu_F^2) f_{b/h_2}(x_2, \mu_F^2) \\ &\times \frac{d\hat{\sigma}_{ab}^{WW}}{dp_T^2}(p_T, M, \hat{s}, \alpha_s(\mu_R^2), \mu_R^2, \mu_F^2), \end{aligned} \quad (2.1)$$

where  $f_{a/h_1}$  and  $f_{b/h_2}$  are the parton distribution functions for the parton species  $a$  and  $b$  in the two colliding hadrons,  $\hat{s} = sx_1x_2$  is the partonic center-of-mass energy, and  $d\hat{\sigma}_{ab}^{WW}/dp_T^2$  is the partonic cross section. The partonic cross section will be the sum of a resummed part and a finite part; the finite part matches resummation with fixed-order calculations. In our case, we will give approximate NNLL + LO results which effectively include the exact LO results at  $O(\alpha_s(\mu_R^2))$  plus approximate NNLL resummation correction terms at  $O(\alpha_s^n(\mu_R^2))$ ,  $2 \leq n \leq \infty$ .

The quantity that is resummed directly is actually the double transform of the partonic cross section,

$$\mathcal{W}_{ab,N}^{WW}(b, M; \alpha_s(\mu_R^2), \mu_R^2, \mu_F^2), \quad (2.2)$$

where  $b$ , the impact parameter, is the Fourier transform moment with respect to  $p_T$ , while  $N$  is the Mellin transform moment with respect to  $z = M/\hat{s}$ . To invert the Mellin transform, we use the standard formula

$$\begin{aligned} \mathcal{W}_{ab}^{WW}(b, M, \hat{s} = M^2/z; \alpha_s(\mu_R^2), \mu_R^2, \mu_F^2) &= \int_{c-i\infty}^{c+i\infty} \frac{dz}{2\pi i} z^{-N} \mathcal{W}_{ab,N}^{WW}(b, M, \alpha_s(\mu_R^2), \mu_R^2, \mu_F^2) \end{aligned} \quad (2.3)$$

where  $c$ , a positive number, is the intercept between the integration contour and the real axis. In numerical implementations, the contour is deformed to the left on both the upper and lower complex planes, leaving the integral invariant but improving numerical convergence. To perform the convolution in Eq. (2.1), we fit the parton distribution functions with simple analytic functions [51] to obtain analytical Mellin transforms. We multiply the Mellin transform of the parton distribution functions with the Mellin transform of the partonic cross section, before we actually invert the transform. The error associated with fitting is less than  $10^{-3}$ .

<sup>1</sup>In our convention, LO  $p_T$  distribution is at the same  $\alpha_s$  order as the NLO total cross section.

To invert the Fourier transform in Eq. (2.1), we use

$$\begin{aligned} & \frac{d\hat{\sigma}_{ab}^{WW}}{dp_T^2}(p_T, M, \hat{s}, \alpha_s(\mu_R^2), \mu_R^2, \mu_F^2) \\ &= \frac{M^2}{\hat{s}} \int \frac{d^2\mathbf{b}}{4\pi} e^{i\mathbf{b}\cdot p_T} \mathcal{W}_{ab}^{WW}(b, M, \hat{s}, \alpha_s(\mu_R^2), \mu_R^2, \mu_F^2) \\ &= \frac{M^2}{\hat{s}} \int \frac{d^2b}{4\pi} \frac{b}{2} J_0(bp_T) \mathcal{W}_{ab}^{WW}(b, M, \hat{s}, \alpha_s(\mu_R^2), \mu_R^2, \mu_F^2). \end{aligned} \quad (2.4)$$

The double transform in Eq. (2.1) contains large logarithms of the form  $\sim \log(Mb)$  which correspond to  $\sim \log(M/p_T)$  before the Fourier transform. Ignoring the finite term from matching to fixed-order results, the large logarithms are resummed to all orders by exponentiation (omitting summation over flavor indices, which is needed when multiple parton flavors mix under DGLAP evolution) [49],

$$\begin{aligned} & \mathcal{W}_{ab,N}^{WW}(b, M; \alpha_s(\mu_R^2), \mu_R^2, \mu_F^2) \\ &= \mathcal{H}_N^{WW}(M, \alpha_s(\mu_R^2); M^2/\mu_F^2, M^2/Q^2) \\ & \quad \times \exp\{\mathcal{G}_N(\alpha_s(\mu_R^2), L; M^2/\mu_R^2, M^2/Q^2)\}, \end{aligned} \quad (2.5)$$

where the  $\mathcal{H}_N^{WW}$  function is only sensitive to physics at the scale comparable with  $M$  and hence does not depend on  $b$ . On the other hand, the function  $\mathcal{G}_N$  is sensitive to physics at the scale of  $1/b \sim p_T$  and is exponentiated to all orders in  $\alpha_s$ . The quantity  $L$  is defined as

$$L \equiv \ln \frac{Q^2 b^2}{b_0^2}, \quad b_0 \equiv 2e^{-\gamma_E} \approx 1.12, \quad (2.6)$$

where  $Q$ , termed the resummation scale, is chosen to be comparable in magnitude to the hard scale of the process. It is an inherent ambiguity in resummation calculations, in addition to the usual  $\mu_R$  and  $\mu_F$  ambiguities for fixed-order calculations.

The exponent in Eq. (2.5) can be expanded in successive logarithmic orders [49,52]

$$\begin{aligned} & \mathcal{G}_N(\alpha_s, L; M^2/\mu_R^2, M^2/Q^2) \\ &= Lg^{(1)}(\alpha_s L) + g_N^{(2)}(\alpha_s L; M^2/\mu_R^2, M^2/Q^2) \\ & \quad + \frac{\alpha_s}{\pi} g_N^{(3)}(\alpha_s L; M^2/\mu_R^2, M^2/Q^2) \\ & \quad + \sum_{n=4}^{+\infty} \left(\frac{\alpha_s}{\pi}\right)^{n-2} g_N^{(n)}(\alpha_s L; M^2/\mu_R^2, M^2/Q^2). \end{aligned} \quad (2.7)$$

This expansion makes sense if we regard  $\alpha_s L$  as of order unity. The  $g^{(1)}$  term is the leading logarithmic term, while  $g^{(2)}$  and  $g^{(3)}$  are the NLL and NNLL terms, and so on. The variation of  $Q$  shuffles terms between the fixed-order and

resummed terms and can give an estimate for as yet uncomputed higher logs.

An alternative representation [48,49] of Eq. (2.7) is (for illustration, we give the expression that is valid when there is a single parton flavor)

$$\begin{aligned} & \mathcal{G}_N(\alpha_s, L; M^2/\mu_R^2, M^2/Q^2) \\ &= - \int_{b_0^2/b^2}^{Q^2} \frac{dq^2}{q^2} \left[ A(\alpha_s(q^2)) \ln \frac{M^2}{q^2} + \tilde{B}_N(\alpha_s(q^2)) \right], \end{aligned} \quad (2.8)$$

$$\tilde{B}_N(\alpha_s) \stackrel{\text{def}}{=} B(\alpha_s) + 2\beta(\alpha_s) \frac{d \ln C_N(\alpha_s)}{d \ln \alpha_s} + 2\gamma_N(\alpha_s), \quad (2.9)$$

where  $A(\alpha_s)$  and  $B(\alpha_s)$  come from the Sudakov form factor, while  $C_N(\alpha_s)$  is related to the perturbative generation of transverse momentum dependent parton distributions from collinear parton distributions and  $\gamma_N(\alpha_s)$  is the moment-space expression for the DGLAP splitting kernel. We include  $A(\alpha_s)$  to  $\alpha_s^3$  order,  $B(\alpha_s)$  to  $\alpha_s^2$  order, the DGLAP splitting kernel  $\gamma_N$  to  $\alpha_s^2$  order (i.e. NLO), and the  $C_N(\alpha_s)$  coefficient to  $\alpha_s$  order. Most of the above ingredients are available in Refs. [48,49], except the  $\alpha_s^3$  order piece of  $A(\alpha_s)$  which is calculated in Ref. [53]. We reused part of the QCD-Pegasus code [54] to calculate the NLO DGLAP splitting kernel in complex moment space. The spin-averaged one-loop virtual correction to  $q\bar{q} \rightarrow W^+W^-$ , computed in Ref. [5], is absorbed into the order  $\alpha_s$  flavor-diagonal part of the  $C_N$  function. We also do not have the full two-loop virtual corrections to the  $q\bar{q} \rightarrow W^+W^-$  amplitude. Therefore, our results have approximate NNLL accuracy.

To ensure that the resummed and matched prediction preserves the NLO total cross section, in Eq. (2.7) we shift  $L$  from the definition Eq. (2.6) to the modified value  $\ln(Q^2 b^2/b_0^2 + 1)$ , which imposes  $G_N = 0$  when  $b = 0$ . This shift does not affect the low  $p_T$  region to leading power in  $p_T/M$ .

## B. Numerical results

The full details about the underlying resummation formalism, in particular the diagonalization of the DGLAP splitting kernel in the multicolor case and the matching to fixed-order calculations, are covered in Refs. [49,50] and will not be repeated here. We now go on to present numerical results. To make sure our numerical implementation is correct, we have reproduced the  $Z$ -boson resummed transverse momentum distribution in Ref. [50], including effects of varying the resummation scale  $Q$ .

We use the MSTW 2008 NLO parton distribution functions [55]. The central scales we use are  $\mu_R = \mu_F = 2m_W$ ,  $Q = m_W$ . In Fig. 1, we plot the resummed, fixed-order, and finite part of the  $W^+W^-$  transverse momentum distribution using central scales for 8 TeV pp collisions to make it easier for future studies to compare



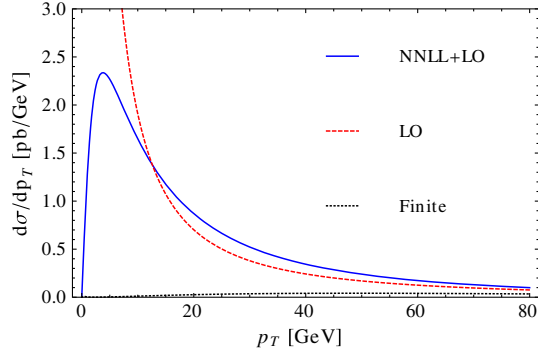


FIG. 1 (color online). Plot of resummed, finite (matching) and fixed-order  $W^+W^-$  transverse momentum distributions from 8 TeV proton collisions. Note that the LO  $p_T$  distribution has the same  $\alpha_s$  order as the NLO total cross section.

results directly. We can see that resummation cures the  $p_T \rightarrow 0$  divergence of the LO distribution and generates substantial corrections. The total cross section obtained from integrating our  $p_T$  distribution agrees with exact fixed-order results to better than 0.5%, which is a consistency check for our numerical accuracy.

To assess perturbative scale uncertainties, we simultaneously vary  $\mu_R$  and  $\mu_F$  up and down by a factor of 2 and separately vary  $Q$  up and down by a factor of 2. The resulting variations in the transverse momentum distributions are plotted in Fig. 2 for 8 TeV collisions. We can see that the largest scale uncertainties result from varying the resummation scale  $Q$ . By adding  $\mu_R$  and  $\mu_F$  variations and  $Q$  variations in quadrature,<sup>2</sup> we produce the distribution with error bands, for 7, 8 and 14 TeV, shown in Fig. 3. if the combined scale uncertainty at the peak of the distribution is around  $\pm 10\%$  for each collision energy.

We now briefly mention nonperturbative effects. In Eq. (2.4)  $\mathcal{W}_{ab}^{WW}$  in fact becomes singular at large  $b$  due to the divergence of the QCD running coupling below the scale  $\Lambda_{\text{QCD}}$ . This is a nonperturbative issue and becomes important at low  $p_T$ . Many prescriptions for regulating the nonperturbative singularity exists, such as the  $b^*$  model [43,47] and the minimal prescription [56]. We adopt a simple cutoff at  $b = 2 \text{ GeV}^{-1}$  for the choice of resummation scale  $Q = 2m_W$  and  $b = 4 \text{ GeV}^{-1}$  for  $Q = m_W$  and  $Q = m_W/2$  and give results both with and without an additional nonperturbative Gaussian smearing factor of  $\exp[-g_{NP}^2 \text{ GeV}^2 b^2]$  with  $g_{NP} = 1$ . The  $W^+W^-$  fiducial cross sections after reweighting parton shower events only differ by about 1% with and without the Gaussian smearing

<sup>2</sup>For example, if the simultaneous variation of  $\mu_R$  and  $\mu_F$  up and down by a factor of 2 produces a variation of  $+a_1/-b_1$ , and similarly the  $Q$  variation produces a variation of  $+a_2/-b_2$ , we take the combined scale uncertainty to be  $+\sqrt{a_1^2 + a_2^2}/-\sqrt{b_1^2 + b_2^2}$ . This procedure for combining uncertainties is used throughout.

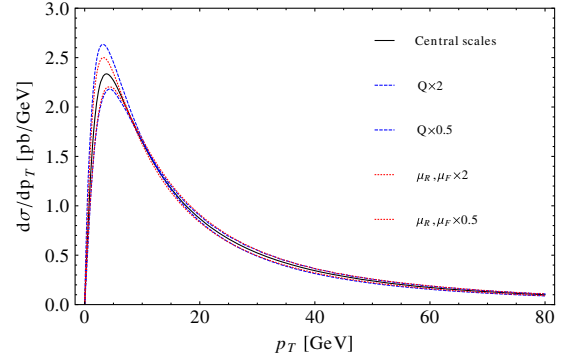


FIG. 2 (color online). Plot of renormalization, factorization and resummation scale variations of the  $W^+W^-$  transverse momentum distribution for 8 TeV collisions.

factor, much smaller than the perturbative scale uncertainties we will encounter. In Fig. 4 we compare the predicted WW transverse momentum distribution with and without the Gaussian smearing factor. The smearing causes the peak to shift by about 0.5 GeV to larger  $p_T$ .

There are of course uncertainties not directly related to our calculation; for instance using different PDF sets can have a few percent effect as demonstrated in Ref. [2]. Since the PDF uncertainties affect both the resummed result and the parton shower result, we expect the effect to largely cancel in the reweighting factor.

Finally, we compare our  $p_T$  distribution at 8 TeV with the soft collinear effective theory (SCET)-based resummation calculation by Ref. [28] in Fig. 5. The results are in good agreement, but our results show a larger error band because we varied both  $\mu_R$  (with  $\mu_F$  locked to be equal to  $\mu_R$ ) and the resummation scale  $Q$ , the latter of which indicates ambiguities in splitting contributions into the resummed part and the finite part, while the calculation by Ref. [28] only considers the variation of one scale.

### III. TRANSVERSE MOMENTUM REWEIGHTING AND FIDUCIAL CROSS SECTIONS

The transverse momentum resummation shown in Sec. II systematically improves our understanding of the  $p_T$  distribution of the diboson system. However, the  $W^+W^-$   $p_T$  distribution as measured by the LHC experiments is not the same as the distribution that is calculated in Sec. II. This is because the detector only measures a certain fiducial region of phase space, there are additional cuts put on the physics objects to reduce backgrounds, and finally there are detector effects which smear the  $p_T$  distribution compared to the theoretical prediction. In very clean channels such as Drell-Yan or ZZ production, these effects can be unfolded more easily, and an unambiguous prediction for the  $p_T$  of the system can be compared to theoretical predictions. For  $W^+W^-$  the effects are more difficult to unfold, and as of yet a full analysis has not been compared to the experimental results for the  $W^+W^-$  diboson system's  $p_T$ . In fact, only

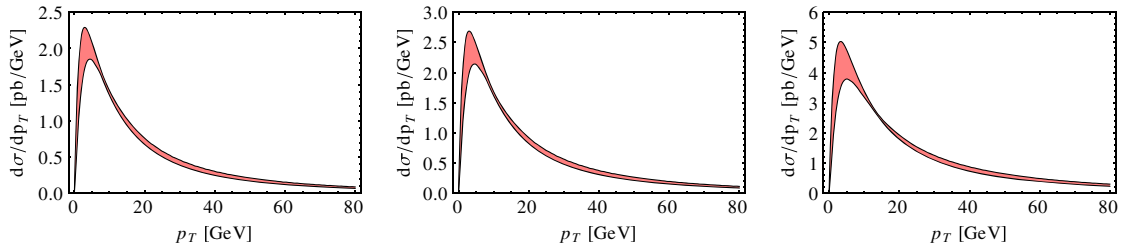


FIG. 3 (color online). NNLO + LO predictions, with error bands, for the  $W^+W^-$  transverse momentum distribution for 7, 8 and 14 TeV collisions.

ATLAS has released a distribution, the vector sum of the  $p_T$  of the leptons and MET, directly correlated to the  $p_T$  of the diboson system.

To compare to data, we must implement the same cuts that the experiments perform. Immediately this runs into potential problems as the distributions predicted in Sec. II are fully inclusive, and even at the leptonic level there are cuts that restrict the distributions to a fiducial phase space. To circumvent these difficulties we implement a reweighting procedure on generated events for the  $p_T$  of the system

prior to cuts and then perform the analysis cuts to find the effects of  $p_T$  resummation. This of course is not a perfect matching of the effects of resummation and data, but without unfolded distributions this is the closest possible comparison that can be made at this point. This procedure is akin to that used for predicting the Higgs signal at the LHC, where the transverse momentum resummed shape, taken from HqT for instance [57], is used to reweight the MC simulated events.

It is possible that a comparison between reweighted events after experimental cuts and the original Monte Carlo events *could* predict the same cross section. The formalism we use by definition does not change the total inclusive cross section. However, if the reweighted distributions that have a different shape are also cut on, then this will affect the total measured cross section. This happens because the cuts change the fiducial cross section and hence the inferred total cross section once the acceptances and efficiencies are unfolded. As we will show, there is not a direct cut on the reweighted  $p_T$  distribution, but the jet-veto cut is highly correlated with it and significantly affects the extrapolated total cross section. Additionally, the cause of the correlation will also reflect that different underlying Monte Carlo generators and parton showers will have different size effects when extrapolating to the total cross section. These differences are demonstrated in Fig. 6 where the  $p_T$  distributions predicted by resummation are compared to

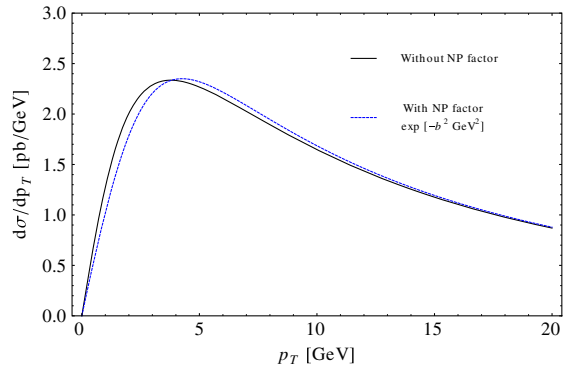


FIG. 4 (color online). NNLL + LO prediction for the WW transverse momentum distribution at 8 TeV, with and without the nonperturbative Gaussian smearing factor  $\exp[-1 \text{ GeV}^2 b^2]$ .

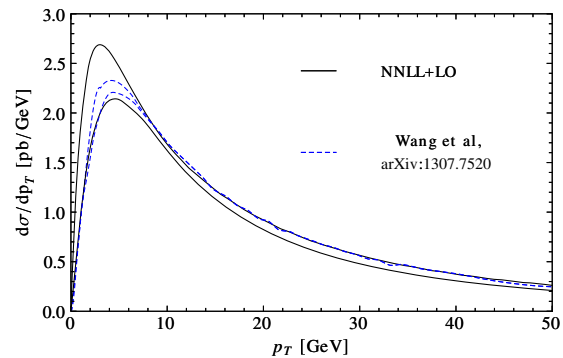


FIG. 5 (color online). Comparison of our resummed WW  $p_T$  distribution with a SCET-based resummation calculation, with error bands shown for both.

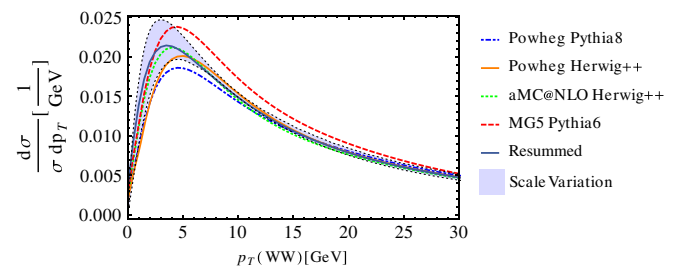


FIG. 6 (color online). Plot of resummation predicted and MC + shower predictions for  $W^+W^-$  transverse momentum distributions at 8 TeV. The shaded region represents the scale  $Q$  variation by a factor of 2 relative to the central scale choice  $Q = m_W$  for the resummation prediction.

TABLE I. ATLAS cut flow for 7 TeV analysis [1].

Exactly two opposite-sign leptons, $p_T > 20$ GeV,
$p_{T\text{leading}} > 25$ GeV
$m_{l'l'} > 15, 15, 10$ GeV (ee, $\mu\mu$ , $e\mu$ )
$ m_{l'l'} - m_Z  > 15, 15, 0$ GeV (ee, $\mu\mu$ , $e\mu$ )
$E_{T,\text{Rel}}^{\text{miss}} > 45, 45, 25$ GeV (ee, $\mu\mu$ , $e\mu$ )
Jet Veto 25 GeV
$p_{Tl'l'} > 30$ GeV

various Monte Carlos (POWHEG BOX [58–60], MadGraph/aMC@NLO and matched Madgraph 0j + 1j [61]) in combination with different parton showers from Herwig ++ [62] and Pythia8[63]. MSTW2008 NLO parton distribution function (pdf) sets were used for all NLO event generations to be consistent with resummation, and the CTEQ6 LO pdf [64] was used for the Madgraph 0 + 1j analysis.

Since the resummation procedure predicts  $p_{T_{ww}}$  shape, we reweight with respect to truth level events, i.e.  $p_{T_{ww}}$ , just after the shower but before detector simulation. To perform the reweighting procedure, resummed theory curves from Sec. II and MC events are binned into 0.5 GeV bins along  $p_{T_{ww}}$ . A reweighting factor is then computed:

$$F[p_T] = \frac{\text{Resummed bin}[p_T]}{\text{MC bin}[p_T]}. \quad (3.1)$$

To approximate detector effects MC events are then smeared using Delphes [65] for a fast detector simulation.<sup>3</sup> Finally, once detector level events are produced we apply the cuts performed by the LHC experiments. An example of the cuts implemented by the ATLAS measurement at 7 TeV is reproduced below in Table I. The cuts from CMS are quite similar, the jet veto as we will show turns out to be the most important effect, and CMS has a jet veto of 30 GeV compared to 25 GeV for ATLAS. We comment on this slight difference in Sec. IV; however, since CMS has not produced a plot of the  $p_T$  of the  $W^+W^-$  system similar to ATLAS, we adopt the ATLAS cuts when demonstrating the effects of using the  $p_T$  resummed reweighted distributions. Pythia8 was used with default tuning, and since all our results are shape dependent, the reweighting procedure should be performed again using our resummation-theory curves when using a nondefault Pythia8 tuning.

<sup>3</sup>The detector simulation is important to match data, as the  $p_T$  distribution of the diboson system predicted by MC@NLO [66] shown by ATLAS cannot be matched without additional smearing of the MET. We demonstrated this with both PGS and Delphes. In the end, however, this smearing does not affect the resummation reweighting effects shown here, because the underlying MC events and resummed reweighted events are affected in the same way. We have demonstrated this explicitly by changing the MET resolution by a factor of 2 each way, which simply shifts the peak of the  $p_T$  distribution.

 TABLE II. Percentage differences of reweighted theory predictions compared to Powheg + Pythia8 at 8 TeV for  $\sigma_{\text{Fid}}$  and various choices of scale. The second column does not include the Gaussian smearing factor for nonperturbative effects, while the third column includes a nonzero nonperturbative factor  $g_{\text{NP}} = 1$  typical for quark dominated initial states.

Scale choice	Difference (%)	Difference with $g_{\text{NP}} = 1$ (%)
Central $\pm$ combined error	$6.5^{+5.0}_{-3.0}$	$6.4^{+5.0}_{-3.0}$
Central scales, $Q = m_W$ ,	6.5	6.4
$\mu_R = \mu_F = 2m_W$		
$Q = 2 \times$ central	5.0	4.8
$Q = 0.5 \times$ central	10.8	10.6
$\mu_R = \mu_F = 0.5 \times$ central	3.9	3.8
$\mu_R = \mu_F = 2 \times$ central	9.2	9.0

 TABLE III. Percentage differences for  $\sigma_{\text{Fid}}$  of reweighted theory predictions compared to MCs + parton showers at 7 TeV.

MC + parton shower	Corrections (%)
Powheg + Pythia8	$6.4^{+4.7}_{-2.8}$
Powheg + Herwig ++	$3.8^{+4.5}_{-2.6}$
aMC@NLO + Herwig ++	$3.3^{+5.0}_{-3.0}$

 TABLE IV. Percentage differences for  $\sigma_{\text{Fid}}$  of reweighted theory predictions compared to MCs + parton showers at 8 TeV.

MC + parton shower	Corrections (%)
Powheg + Pythia8	$6.5^{+5.0}_{-3.0}$
Powheg + Herwig ++	$3.8^{+4.3}_{-2.5}$
aMC@NLO + Herwig ++	$3.1^{+5.0}_{-3.0}$
MADGRAPH LO + Pythia6	$-9.6^{+4.4}_{-2.7}$

 TABLE V. Percentage differences for  $\sigma_{\text{Fid}}$  of reweighted theory predictions compared to MCs + parton showers at 14 TeV.

MC + parton shower	Corrections (%)
Powheg + Pythia8	$7.0^{+6.4}_{-5.1}$
Powheg + Herwig ++	$4.4^{+5.9}_{-4.7}$
aMC@NLO + Herwig ++	$4.2^{+6.5}_{-5.2}$

## A. Reweighting results

We perform the reweighting as described above using a central scale  $Q = m_W$  as well as varying the resummation scale  $Q$  up and down by a factor of 2 while keeping  $\mu_R$  and  $\mu_F$  fixed. We define the percentage difference caused by reweighting as

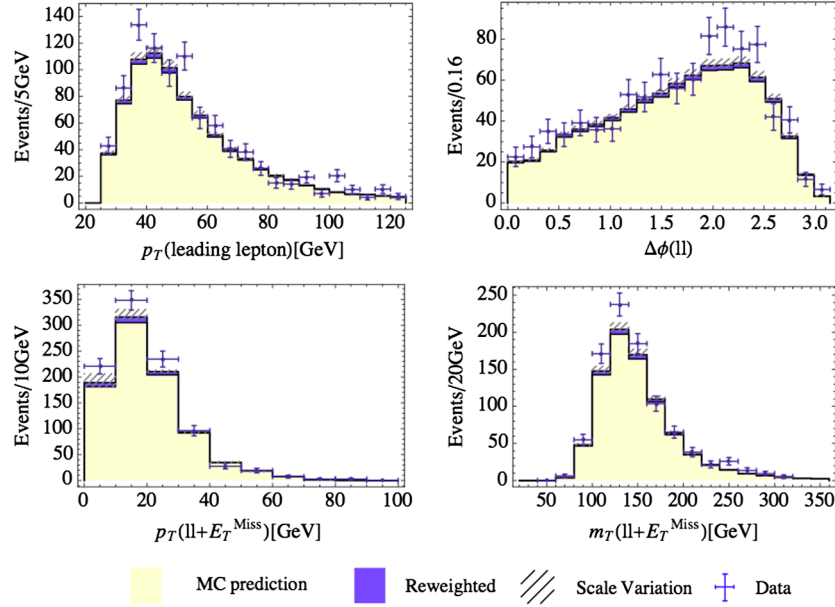


FIG. 7 (color online). aMC@NLO + Herwig ++ observables histogrammed for  $W^+W^-$  transverse momentum distribution for 7 TeV collisions and including the reweighting correction.

$$\text{percentage difference} = \frac{(\text{events}_{\text{res}} - \text{events}_{\text{MC}}) \cdot 100}{\text{events}_{\text{MC}}}, \quad (3.2)$$

where

- (i)  $\text{events}_{\text{MC}}$  is events predicted by the MC before reweighting,
- (ii)  $\text{events}_{\text{res}}$  is events after reweighting the MC events, with a positive percentage difference implying an increase in the theoretical prediction on  $\sigma_{\text{Fid}}$ . To demonstrate

the effects of other scale variations on  $\sigma_{\text{Fid}}$  we also varied  $\mu_R$  and  $\mu_F$  as well as the nonperturbative factor discussed in Sec. II and report the percentage differences compared to Powheg + Pythia8 (8 TeV) as an example in Table II.

We find that, as observed in Sec. II, the Q variation leads to a larger percentage difference than the  $\mu_F$  or  $\mu_R$  scale variation. The nonperturbative factor  $g_{\text{NP}}$  shifts the peak of the underlying  $p_T$  distributions slightly, but in the end has a minimal effect on the cross section. We show the effects of

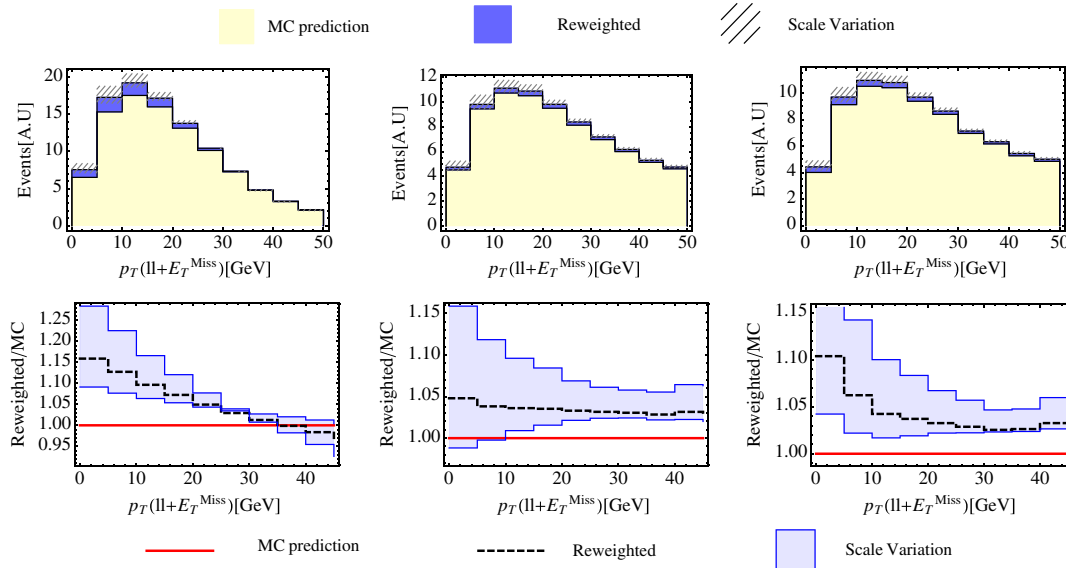


FIG. 8 (color online). The top row shows the reweighting correction for left (Powheg + Pythia8), center (aMC@NLO + Herwig ++), and right (Powheg + Herwig ++ to the  $p_T(ll + E_T^{\text{miss}})$  observables. The bottom row has bin-by-bin percentage difference in events between reweighting and the MC + PS.



TABLE VI. Percentage increase due to resummation-reweighting ( $Q = \frac{m_W}{2}$ ,  $\mu_R = \mu_F = 2m_W$ ) compared to Powheg-Pythia8 at 8 TeV for each cut stage in the cut flows listed from Table I. All percentages are cumulative showing that the jet veto is the largest effect.

Cut	Difference (%)
Exactly two opposite-sign leptons, $p_T > 20$ GeV, $p_{T\text{leading}} > 25$ GeV	1.36
$m_{ll'}$ cuts	1.16
$E_{T,\text{Rel}}^{\text{miss}}$	0.83
Jet veto	9.72
$p_{Tll'}$	10.75

reweighting on MC generators and parton showers in Tables III, IV, and V for 7, 8, and 14 TeV, respectively.

To demonstrate the effects on differential distributions, we use the ATLAS cut flows and show the predictions of  $p_T$  resummation for the 7 TeV ATLAS study [1] compared to the original MC@NLO + Herwig ++ results used by ATLAS. In Fig. 7, we plot the four distributions shown in Ref. [1]. As can be seen in Fig. 7,  $p_T$  reweighting can improve the differential distributions somewhat but is not capable of explaining the full discrepancy using a central choice of scales. With further statistics at the next run it would be useful for the experiments to start to quantify these shape discrepancies rather than simply reporting the total cross section.

To demonstrate the effects at 8 TeV we show the distribution most affected,  $p_T(ll + E_T^{\text{miss}})$ , in Fig. 8 using the same cut flows and different generators. This distribution is directly correlated with the  $p_T$  of the diboson system predicted by resummation and shows the variation compared to MC generators + parton showers. The largest discrepancy compared to MC comes from the use of Powheg + Pythia8, while both Powheg and aMC@NLO are in much better agreement when Herwig ++ is used as the parton shower. However, this does not mean the effects of the parton shower are the sole cause of the discrepancy. In the fractional difference shown in Fig. 8, we see the roughly the same shape dependence for both Powheg curves, but the overall magnitude is reduced for Powheg + Herwig ++ compared to Powheg + Pythia8.

### B. Jet veto

As we have shown thus far, even though the inclusive total cross sections are the same by design, there are appreciable corrections to the fiducial cross section after reweighting. This means that some of the cuts are well correlated with the  $p_{TWW}$  variable and seem to preferentially select the low  $p_{TWW}$  region where the resummation curve dominates all the MCs except Madgraph LO. The percentage change due to reweighting at each cut level was analyzed, and as an example the effects of reweighting at

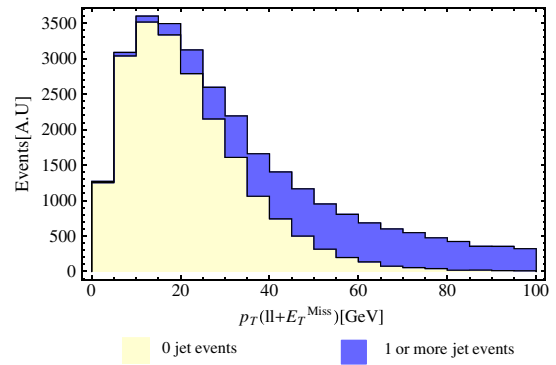


FIG. 9 (color online). Events before the jet veto. The number of 0-jet events or events with one or more jets is shown as a function of the  $p_T$  of the diboson system. Since one or more jet events are vetoed, this sculpts the  $p_T$  shape.

each state in the cut flow is shown for Powheg-Pythia8 at 8 TeV in Table VI. The jet-veto stage is the largest contributor to the reweighting excess. To explicitly check this, the order of the jet veto and  $p_{Tll}$  cuts was reversed, and the biggest jump was found to still be the jet-veto cut. In Fig. 9 we show the correlation between 0-jet events and  $> 0$  jet events as a function of  $p_T(ll + E_T^{\text{miss}})$  before the jet veto is applied. Note that in Fig. 9, 0-jet events primarily comprise the low  $p_T$  of the diboson system, and as such a jet veto implies that the fiducial cross section will become more sensitive to the shape given by  $p_T$  resummation. This clearly points to the jet-veto cut as the major contributor to changes in the fiducial cross section from  $p_T$  resummation reweighting. If the jet veto were increased this result would still hold; however, the 0-jet cross section would then be integrated over a larger range of  $p_T$  for the diboson, and thus there would be a smaller effect on the fiducial cross section. In particular, if the jet veto were dropped entirely this would be equivalent to integrating over the entire diboson  $p_T$  which by definition would not change the measured cross section.

## IV. DISCUSSION

As we have shown,  $p_T$  resummation, when used to reweight NLO MC distributions, can have a sizable effect on the predicted fiducial and the inferred total cross sections. The general trend in comparison with Monte Carlo generators and parton showers is to increase the predicted cross section  $\sim 3-7\%$  and thus decrease the observed discrepancy compared to ATLAS and CMS. Our change in the predicted cross section and differential distributions depends on the choice of resummation scale for the  $W^+W^-$  final state of which the uncertainty is not accounted for in fixed-order + parton shower calculations. At large  $p_T$  the fixed-order calculation is valid, while at small to moderate  $p_T$  the resummation calculation is most reliable. This scale in practice is analogous to the matrix element-parton shower matching scale when implementing

matching procedures between the two. As discussed in Sec. II, the resummation scale should be similar to the other hard scales in the problem. We have chosen the simple scale choice, analogous to what is done for Drell-Yan[50,67], of  $\sim M/2$ , which for the  $W^+W^-$  process we have approximated as the fixed scale  $Q = M_W$ . We have demonstrated that the variation in this scale actually can imply quite a deal of uncertainty. For instance at 8 TeV using Powheg + Pythia8, by varying  $Q$  by a factor of 2 each time we introduce a variation on the measured cross section  $\sim \pm 3\%$ .

Given that there is no *a priori* correct choice of the scale  $Q$ , a question naturally arises whether one can simply choose a scale to match the experimental data presented thus far. It is important to note that the measurements presented thus far have used *different* event generators and parton showers. For instance the preliminary result at 8 TeV by CMS [4] used Madraph LO + Pythia6, whereas the ATLAS full luminosity result [2] used Powheg + Pythia8. As shown in Table IV, the excess shown by CMS should be even *larger* based on our results, while the ATLAS discrepancy should be reduced as mentioned above. Therefore, even if a single scale were chosen for the results thus far, it would not imply that it could put both experiments results into better agreement with the SM. However, if a consistent choice of generator were implemented, we could in principle address the question of choosing a scale that is best for this process.

If one chooses a best-fit scale  $Q$  to fit the experimental discrepancy in  $W^+W^-$  data there are potential implications elsewhere. Given that the premise behind resummation is that it should be approximately factorized from the hard process, if the initial partons for two processes are the same and there are no colored particles that are exclusively identified in the final state, the effects of resummation should be universal for different processes with similar scales. Thus, if there is a “correct” choice of scale for the  $W^+W^-$  process, then this choice of scale should be implemented for  $W^\pm Z$  and  $ZZ$  diboson processes as well, because of the similar hard scales in these diboson systems. The  $W^\pm Z$  and  $ZZ$  processes are experimentally even easier channels, especially the  $ZZ$  channel where the  $p_T$  of the  $ZZ$  system can be reconstructed with less uncertainty. The drawback of course is the reduced number of events in these channels, but nevertheless statistics are starting to approach the point where a useful comparison can be made, e.g. the recent CMS 8 TeV measurement [4]. The  $ZZ$  cross section and  $p_T$  distribution [68] are in remarkable agreement with the SM, and as such if there were a large change in the  $p_T$  distribution caused by the use of the best-fit  $W^+W^-$  scale  $Q$  then it would cause the agreement with the SM of  $ZZ$  to become worse. However, we note that the change from  $p_T$  resummation in the  $W^+W^-$  process is mostly due to the imposition of a jet veto which the  $ZZ$  channel does not have. We find that choosing a scale that

fits the  $W^+W^-$  discrepancy and naively calculating the inclusive change for  $ZZ$  causes a disagreement with data in all  $p_T$  bins. Further study of course is warranted, and a simultaneous fit should be employed to understand the agreement between the SM and measured diboson processes. This of course brings up a more general point that, in analyzing the agreement between the SM and LHC data, similar theoretical methods should be employed and not just a choice of what fits best for a given process. The understanding of the different choices made by experiments contains important theoretical information about the SM, and in the worst-case scenario new physics could be inadvertently missed being discovered.

Another important lesson reemphasized by this study is the need for further theoretical investigations of jet vetos. As we have shown  $p_T$  resummation causes a sizable effect on the total cross section because of the interplay between the jet veto and the  $p_T$  distribution. Clearly the correlation demonstrated in Sec. III, especially Fig. 9, shows that the effects calculated in jet-veto resummation should be well approximated by the method employed here, similar to what was shown in Ref. [31]. Of course there are additional logs related to the jet veto which cannot be systematically improved upon within  $p_T$  resummation. However, the distributions shown in Figs. 7 and 8 cannot be reproduced in jet-veto resummation alone, whereas our methods can. It would be interesting to further investigate the interplay of these two types of resummation and the reweighting of parton showered events for more processes.

Another interesting question associated with the jet veto is how the LHC experiments can test the effects of the jet veto on the  $W^+W^-$  cross section measurement. The jet veto is a necessary evil in the context of measuring  $W^+W^-$  without being overwhelmed by  $t\bar{t}$ . However, if the jet veto were weakened significantly, then the effects demonstrated in this paper would disappear both in the context of  $p_T$  resummation and jet-veto resummation. If the jet veto were varied, this could be compared to definitive predictions for the cross section as a function of the jet veto. To alleviate the issue of the  $t\bar{t}$  background, we suggest that the experiments separately implement a b-jet veto and a light jet veto, of which the light jet veto should be varied to study its effects.

In this paper we have not explicitly demonstrated the effects of resummation on the contribution of  $gg \rightarrow W^+W^-$  to the  $W^+W^-$  cross section. This contribution is a small fraction of the total cross section, and as such, even though resummation effects will modify its shape as well, it will not change our conclusions. However, it is important to note that the peak of the  $p_T$  spectrum for  $gg \rightarrow W^+W^-$  should be at approximately 10 GeV higher than for quark initiated  $W^+W^-$ , as is generic for  $gg$  initiated processes, in e.g. Ref. [49]). For a sufficiently precise measurement of the  $p_T$  distribution it would be necessary to have the shape of this distribution correct as well. A more interesting

direction is the implications of understanding the correct shape of the SM  $W^+W^-$  production background for the extraction of the Higgs signal in the  $H \rightarrow W^+W^-$  decay channel. Given that the  $W^+W^-$  background is extracted via data-driven methods, it is important that the shape of the distributions of the  $W^+W^-$  background is known when extrapolating from control to signal regions. While the  $p_T$  of the  $W^+W^-$  system is not a variable used for the signal/control regions, as shown in our results for the reweighted kinematic distributions at 7 TeV, there is a non-negligible effect on the shape of relevant variables. Future investigation is needed to study the effects of resummation on the measured signal strength of the Higgs in the  $W^+W^-$  channel.

There are other avenues for future study, for instance investigating simultaneous resummation of  $W^+W^- p_T$  with other observables, such as rapidity, to determine if any of the other cuts put on the fiducial phase space could alter the extraction of a total cross section. Regardless of future direction, this work has clearly demonstrated the

importance of  $p_T$  resummation when combined with fiducial phase space cuts. Similar to how the  $p_T$  distribution of the Higgs signal is reweighted to make precise predictions for Higgs physics, it is important to use the correct  $p_T$  shape when considering processes where the  $W^+W^-$  signal is either being measured or is an important background. To help facilitate future studies we plan to distribute the underlying  $p_T$  resummed distributions used in this study to any group interested in using them via a website.

## ACKNOWLEDGMENTS

We would like to thank Karen Chen, David Curtin, Rafael Lopes de Sa, Dmytro Kovalskyi, Marc-Andre Pleier, Ted Rogers, and George Sterman for helpful discussions. The work of P. M. was supported in part by NSF CAREER Grant No. NSF-PHY-1056833. The work of H. R. and M. Z. was supported in part by NSF Grant No. PHY-1316617.

- 
- [1] ATLAS Collaboration, *Phys. Rev. D* **87**, 112001 (2013).
  - [2] ATLAS Collaboration, Report No. ATLAS-CONF-2014-033.
  - [3] S. Chatrchyan *et al.* (CMS Collaboration), *Eur. Phys. J. C* **73**, 2610 (2013).
  - [4] S. Chatrchyan *et al.* (CMS Collaboration), *Phys. Lett. B* **721**, 190 (2013).
  - [5] S. Frixione, *Nucl. Phys.* **B410**, 280 (1993).
  - [6] J. Ohnemus, *Phys. Rev. D* **44**, 1403 (1991).
  - [7] S. Chatrchyan *et al.* (CMS Collaboration), *J. High Energy Phys.* **01** (2014) 096.
  - [8] ATLAS Collaboration, *Phys. Lett. B* **726**, 88 (2013).
  - [9] G. Davatz, G. Dissertori, M. Dittmar, M. Grazzini, and F. Pauss, *J. High Energy Phys.* **05** (2004) 009.
  - [10] D. Curtin, P. Jaiswal, and P. Meade, *Phys. Rev. D* **87**, 031701 (2013).
  - [11] D. Curtin, P. Jaiswal, P. Meade, and P.-J. Tien, *J. High Energy Phys.* **08** (2013) 068.
  - [12] K. Rolbiecki and K. Sakurai, *J. High Energy Phys.* **09** (2013) 004.
  - [13] D. Curtin, P. Meade, and P.-J. Tien, [arXiv:1406.0848](https://arxiv.org/abs/1406.0848).
  - [14] J. S. Kim, K. Rolbiecki, K. Sakurai, and J. Tattersall, [arXiv:1406.0858](https://arxiv.org/abs/1406.0858).
  - [15] P. Jaiswal, K. Kopp, and T. Okui, *Phys. Rev. D* **87**, 115017 (2013).
  - [16] N. Kauer and G. Passarino, *J. High Energy Phys.* **08** (2012) 116.
  - [17] N. Kauer, *J. High Energy Phys.* **12** (2013) 082.
  - [18] F. Campanario, M. Rauch, and S. Sapeta, *Nucl. Phys.* **B879**, 65 (2014).
  - [19] F. Campanario and S. Sapeta, *Phys. Lett. B* **718**, 100 (2012).
  - [20] F. Cascioli, S. Hoeche, F. Krauss, P. Maierher, S. Pozzorini, and F. Siegert, *J. High Energy Phys.* **01** (2014) 046.
  - [21] M. Bonvini, F. Caola, S. Forte, K. Melnikov, and G. Ridolfi, *Phys. Rev. D* **88**, 034032 (2013).
  - [22] F. Cascioli, T. Gehrmann, M. Grazzini, S. Kallweit, P. Maierhöfer, A. von Manteuffel, S. Pozzorini, D. Rathlev, L. Tancredi, and E. Weihs, *Phys. Lett. B* **735**, 311 (2014).
  - [23] S. Dawson, I. M. Lewis, and M. Zeng, *Phys. Rev. D* **88**, 054028 (2013).
  - [24] L. Magnea and G. F. Sterman, *Phys. Rev. D* **42**, 4222 (1990).
  - [25] V. Ahrens, T. Becher, M. Neubert, and L. L. Yang, *Phys. Rev. D* **79**, 033013 (2009).
  - [26] V. Ahrens, T. Becher, M. Neubert, and L. L. Yang, *Eur. Phys. J. C* **62**, 333 (2009).
  - [27] M. Grazzini, *J. High Energy Phys.* **01** (2006) 095.
  - [28] Y. Wang, C. S. Li, Z. L. Liu, D. Y. Shao, and H. T. Li, *Phys. Rev. D* **88**, 114017 (2013).
  - [29] V. M. Abazov *et al.* (D0 Collaboration), *Phys. Rev. D* **89**, 012005 (2014).
  - [30] D. de Florian, G. Ferrera, M. Grazzini, and D. Tommasini, *J. High Energy Phys.* **11** (2011) 064.
  - [31] A. Banfi, G. P. Salam, and G. Zanderighi, *J. High Energy Phys.* **06** (2012) 159.
  - [32] A. Banfi, P. F. Monni, G. P. Salam, and G. Zanderighi, *Phys. Rev. Lett.* **109**, 202001 (2012).
  - [33] C. F. Berger, C. Marcantonini, I. W. Stewart, F. J. Tackmann, and W. J. Waalewijn, *J. High Energy Phys.* **04** (2011) 092.
  - [34] F. J. Tackmann, J. R. Walsh, and S. Zuberi, *Phys. Rev. D* **86**, 053011 (2012).
  - [35] I. W. Stewart, F. J. Tackmann, J. R. Walsh, and S. Zuberi, *Phys. Rev. D* **89**, 054001 (2014).

- [36] T. Becher and M. Neubert, *J. High Energy Phys.* **07** (2012) 108.
- [37] T. Becher, M. Neubert, and L. Rothen, *J. High Energy Phys.* **10** (2013) 125.
- [38] I. Moulst and I. W. Stewart, *J. High Energy Phys.* **09** (2014) 129.
- [39] Y. L. Dokshitzer, D. Diakonov, and S. I. Troian, *Phys. Lett.* **79B**, 269 (1978).
- [40] G. Parisi and R. Petronzio, *Nucl. Phys.* **B154**, 427 (1979).
- [41] G. Curci, M. Greco, and Y. Srivastava, *Nucl. Phys.* **B159**, 451 (1979).
- [42] J. C. Collins and D. E. Soper, *Nucl. Phys.* **B193**, 381 (1981); **B213**, 545(E) (1983).
- [43] J. C. Collins and D. E. Soper, *Nucl. Phys.* **B197**, 446 (1982).
- [44] J. Kodaira and L. Trentadue, *Phys. Lett.* **112B**, 66 (1982).
- [45] J. Kodaira and L. Trentadue, *Phys. Lett.* **123B**, 335 (1983).
- [46] G. Altarelli, R. K. Ellis, M. Greco, and G. Martinelli, *Nucl. Phys.* **B246**, 12 (1984).
- [47] J. C. Collins, D. E. Soper, and G. F. Sterman, *Nucl. Phys.* **B250**, 199 (1985).
- [48] S. Catani, D. de Florian, and M. Grazzini, *Nucl. Phys.* **B596**, 299 (2001).
- [49] G. Bozzi, S. Catani, D. de Florian, and M. Grazzini, *Nucl. Phys.* **B737**, 73 (2006).
- [50] G. Bozzi, S. Catani, G. Ferrera, D. de Florian, and M. Grazzini, *Phys. Lett. B* **696**, 207 (2011).
- [51] D. de Florian and J. Zurita, *Phys. Lett. B* **659**, 813 (2008).
- [52] S. Catani, D. de Florian, M. Grazzini, and P. Nason, *J. High Energy Phys.* **07** (2003) 028.
- [53] T. Becher and M. Neubert, *Eur. Phys. J. C* **71**, 1665 (2011).
- [54] A. Vogt, *Comput. Phys. Commun.* **170**, 65 (2005).
- [55] A. D. Martin, W. J. Stirling, R. S. Thorne, and G. Watt, *Eur. Phys. J. C* **63**, 189 (2009).
- [56] E. Laenen, G. F. Sterman, and W. Vogelsang, *Phys. Rev. Lett.* **84**, 4296 (2000).
- [57] G. Bozzi, S. Catani, D. de Florian, and M. Grazzini, *Phys. Lett. B* **564**, 65 (2003); *Nucl. Phys.* **B737**, 73 (2006); D. de Florian, G. Ferrera, M. Grazzini, and D. Tommasini, *J. High Energy Phys.* **11** (2011) 064.
- [58] P. Nason, *J. High Energy Phys.* **11** (2004) 040.
- [59] S. Frixione, P. Nason, and C. Oleari, *J. High Energy Phys.* **11** (2007) 070.
- [60] S. Alioli, P. Nason, C. Oleari, and E. Re, *J. High Energy Phys.* **06** (2010) 043.
- [61] J. Alwall, R. Frederix, S. Frixione, V. Hirschi, F. Maltoni, O. Mattelaer, H.-S. Shao, T. Stelzer, P. Torrielli, and M. Zaro, *J. High Energy Phys.* **07** (2014) 079.
- [62] M. Bahr *et al.*, *Eur. Phys. J. C* **58**, 639 (2008).
- [63] T. Sjostrand, S. Mrenna, and P. Z. Skands, *J. High Energy Phys.* **05** (2006) 026.
- [64] J. Pumplin, D. R. Stump, J. Huston, H. L. Lai, P. M. Nadolsky, and W. K. Tung, *J. High Energy Phys.* **07** (2002) 012.
- [65] J. de Favereau, C. Delaere, P. Demin, A. Giammanco, V. Lemaître, A. Mertens, and M. Selvaggi, *J. High Energy Phys.* **02** (2014) 057.
- [66] S. Frixione and B. R. Webber, *J. High Energy Phys.* **06** (2002) 029.
- [67] G. Bozzi, S. Catani, G. Ferrera, D. de Florian, and M. Grazzini, *Nucl. Phys.* **B815**, 174 (2009).
- [68] V. Khachatryan *et al.* (CMS Collaboration), [arXiv: 1406.0113](https://arxiv.org/abs/1406.0113).